ACS APPLIED MATERIALS & INTERFACES

Research Article

www.acsami.org

Lotus-Leaf-Like Topography Predominates over Adsorbed ECM Proteins in Poly(3-hydroxybutyrate-*co*-3-hydroxyhexanoate) Surface/Cell Interactions

Jun Zheng,[†,‡] Dan Li,*[,†] Lin Yuan,[†] Xiaoli Liu,[†] and Hong Chen*[,†]

[†]Jiangsu Key Laboratory of Advanced Functional Polymer Design and Application, The Key Lab of Health Chemistry and Molecular Diagnosis of Suzhou, College of Chemistry, Chemical Engineering and Materials Science, Soochow University, Suzhou 215123, People's Republic of China

[‡]School of Materials Science and Engineering, Wuhan University of Technology, Wuhan 430070, People's Republic of China

ABSTRACT: It is well-known that extracellular matrix (ECM) proteins mediate cell/surface interactions. However, introduction of a specific surface topography may disturb the correlation between ECM proteins adsorption and cells adhesion on a given surface. In present study, lotus-leaf-like topography was introduced on the surface of a biodegradable material, poly(3-hydroxybutyrate-*co*-3-hydroxyhexanoate) (PHBHHx). Protein adsorption and cell interactions with this lotus-leaf-like surface (designated PHBHHx-L) were investigated. Water contact angle data indicated that the hydrophobicity of PHBHHx was enhanced by the introduction of lotus-leaf-like topography. The adsorption of extracellular matrix proteins (fibronectin and vitronectin) on PHBHHx-L was measured by enzyme linked immunosorbent assay (ELISA). Compared with flat PHBHHx, adsorption on the PHBHHx-L surface increased by ~260% for fibronectin and ~40% for vitronectin. In contrast, fibroblast and endothelial cell adhesion and proliferation were reduced on the PHBHHx-L compared to the flat polymer surface. These results suggest that the inhibition of cell adhesion and proliferation caused by the lotus-leaf-like topography dominates over the effect of the adsorbed adhesive proteins in promoting adhesion and proliferation. It can be concluded that the lotus-leaf-like topography plays a dominant role in cell/PHBHHx-L interactions. The present findings indicate the complexity of the interplay among surface topography, adsorbed proteins, and cell−surface interactions.

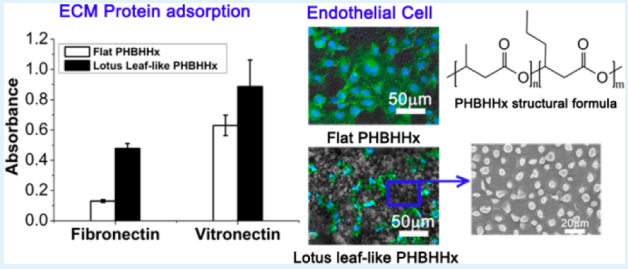

KEYWORDS: *poly(3-hydroxybutyrate-co-3-hydroxyhexanoate), lotus-leaf-like, surface topography, protein adsorption, cell proliferation*

1. INTRODUCTION

Reticulated extracellular matrix (ECM), consisting of cell-secreted proteins and polysaccharides with a complex micrometer- and submicrometer-scale, three-dimensional structure, is an important microenvironment for cell survival.[1−3] Cells respond to these topographical structures and exhibit different behavior on different topographies.[4−6] In the fields of biomaterials and tissue engineering, it is of great importance to study the effects of surface topography on cell behavior, including cell adhesion, migration, proliferation, secretion and gene expression.

Surface-adsorbed proteins play an important role in the interactions of materials and cells. Proteins adsorb to material surfaces within seconds upon exposure to a biological environment.[7] Cells then adhere and proliferate via interactions between integrin receptors in the cell membrane and adsorbed extracellular matrix proteins.[7] Many reports have suggested that surface topography influences cell/surface interactions via adsorbed proteins. For example, Shi et al. found that surface topography promoted cell adhesion only in the presence of cell-adhesive proteins, indicating that the proteins were essential for cell adhesion.[8] Deligianni et al. found that fibronectin adsorption on a titanium alloy increased as the surface roughness increased, possibly accounting for the concomitant increase in cellular attachment.[9] It was also reported that the microstructured surface indirectly influenced the location of adherent platelets by affecting the distribution of adsorbed fibrinogen.[10]

Other researchers have suggested that there is no direct correlation between cell-adhesive protein adsorption and cell adhesion on topographical surfaces.[11,12] For instance, on a microgrooved surface overlaid with a fibronectin pattern orthogonal to the grooves, the cells aligned preferentially with the grooves, not the fibronectin.[13] Also, rougher surfaces showed higher fibronectin adsorption but lower cell adhesion,[14] implying that the quantity of adsorbed fibronectin does not directly determine the cell response.

Received: May 8, 2013
Accepted: May 30, 2013
Published: May 30, 2013

In addition, surface chemical composition can also dramatically influence the interactions of cells with topographical surfaces.[15−17] Consequently, the effect of surface topography on cell behavior is difficult to determine: for example materials with the same surface topography, but different chemical composition may show different cell interactions and different contributions of protein adsorption to these interactions.

The aim of the present study was to investigate the effects of lotus-leaf-like topography on the interactions of cells with poly(3-hydroxybutyrate-*co*-3-hydroxyhexanoate) (PHBHHx). PHBHHx, produced by bacteria, is a novel polyester with general biodegradability[18,19] and good biocompatibility,[20,21] and has potential for use as a scaffold in tissue engineering.[22] In this work, chemically homogeneous lotus-leaf-like topography on PHBHHx was achieved by replica molding, and the effects of this topography on cell adhesion and proliferation were investigated. The contribution of cell-adhesive protein adsorption to cell interactions was a major focus. The results of this study may provide guidance for the design of PHBHHx as tissue engineering scaffolds.

2. EXPERIMENTAL SECTION

2.1. Materials. Poly(3-hydroxybutyrate-*co*-3-hydroxyhexanoate) (PHBHHx, M_w 310 000 Da; 16% HHx) was kindly provided by Professor Chen GQ, Tsinghua University. Sylgard 184 was purchased from Dow Corning (Midland, MI, USA). Methyl thiazolyltetrazolium (MTT) and 4-nitrophenyl phosphate disodium (pNPP) were from Amresco (Solon, OH, USA). Fibrinogen (Fg) and bovine serum albumin (BSA) were from Sigma (St. Louis, MO, USA). Rabbit antifibronectin and rabbit antivitronectin were from Trevigen. Inc. (Gaithersburg, MD, USA). Alkaline phosphatase (AP) conjugated sheep antirabbit IgG was from Boster Biological Technology, Ltd. (Wuhan, China). L929 cells and human umbilical vein endothelial cells (HUVEC) were purchased from the China Center for Type Culture Collection (Wuhan, China). *N*,*N*-Dimethylformamide (DMF) and other reagents were from Sinopharm Chemical Reagent Corporation (Shanghai, China). Millipore Water (18 MΩ cm) was used in all experiments.

2.2. Preparation and Characterization of Lotus-leaf-like PHBHHx Films. Lotus leaf negative template was prepared as previously described.[15] Briefly, a piece of fresh natural lotus leaf was placed on the bottom of a polystyrene plate (6 cm in dameter). PDMS prepolymer was then added to cover the lotus leaf. After curing, the PDMS layer, with topography complementary to that of the lotus leaf, was peeled off. This PDMS film is referred to as the negative template.

PHBHHx was dissolved in DMF at 60 °C (3 h incubation). The solution was layered on the PDMS negative template and degassed for 1 h under vacuum. The solvent was slowly evaporated at 60 °C for 40 h in an air oven, and then under vacuum for 5 days. The film, with lotus-leaf-like topography, designated PHBHHx-L, was then separated from the PDMS. PHBHHx flat surface (designated PHBHHx-F) was prepared by casting from PHBHHx solution on a clean glass Petri dish following the same procedure as for PHBHHx-L. Films ∼6.34 mm in diameter and ∼0.12 mm thick were punched, rinsed with ethanol, and vacuum-dried for 24 h at 40 °C.

Advancing and receding water contact angles were measured using an SL200C automatic contact angle meter (USA KINO Industry Co., NY, USA) with a drop volume of 6 μL. Three films of each sample were used for the measurements. Surface morphology was observed by scanning electron microscopy (SEM, S-4700, Hitachi).

2.3. Protein Adsorption. *2.3.1. Fibrinogen Adsorption from Buffer.* Fibrinogen (Fg) was labeled with ^{125}I (Chengdu Gaotong Isotope Co., Ltd., China) using the ICl method.[23] Labeled Fg was mixed with unlabeled Fg (1:19, labeled:unlabeled) at a total concentration of 1 mg/mL. Samples were incubated with Fg in phosphate buffered saline (PBS, pH 7.4) for 3 h at room temperature, then rinsed three times with PBS, wicked onto filter paper, and transferred to clean tubes for radioactivity determination using a Wizard 3 in. 2480 Automatic Gamma Counter (PerkinElmer Life Sciences, Shelton, CT). Radioactivity was converted to protein amount.

2.3.2. Fibronectin and Vitronectin Adsorption from Cell Culture Medium. Fibronectin (Fn) and vitronectin (Vn) adsorption were measured by enzyme linked immunosorbent assay (ELISA). Films were placed in 96-well EIA/RIA plates (Corning, MA, USA). Cell culture medium (250 μL) containing 10% fetal bovine serum (FBS) was added to each well and a well without FBS was used as control. FBS contains a variety of proteins, including Fn and Vn. After incubation at 37 °C for 3 h, the films were rinsed three times with PBS and blocked with 1% BSA at 37 °C for 1.5 h. After rinsing with TBST (Tris buffered saline containing 0.05% Tween-20), the films were incubated with rabbit antibovine Fn/Vn antibody in TBST (dilution of 1:10,000) at 37 °C for 1 h. After rinsing with TBST, the films were incubated with alkaline phosphatase-conjugated sheep antirabbit IgG in TBST (dilution of 1:10 000) at 37 °C for 1 h. The films were rinsed, transferred to new wells containing substrate solution (*p*-nitrophenyl phosphate, 1 mg/mL), and incubated at room temperature in the dark. The reaction was stopped by adding 1N NaOH. One-hundred-fifty microliters of the solution was pipetted from each well into new wells, and the absorbance at 405 nm was determined (Thermo Scientific Varioskan Flash, Thermo scientific, USA).

2.4. Cell Adhesion and Proliferation. Fibroblasts (L929) and endothelial cells (HUVEC) were cultured in RPMI medium 1640 (Hyclone, UT, USA) containing 10% FBS, 100 U/mL penicillin, and 0.1 mg/mL streptomycin at 37 °C with 98% humidity and 5% CO_2 in air. Cells were harvested by trypsinization at approximately 80−90% confluence.

The films were carefully placed on the bottom of the wells of a 24-well tissue culture plate with the lotus-leaf-like topography facing up. The plates were sterilized with 75% ethanol for 30 min and then washed with sterile PBS. The cells were seeded at a density of 5×10^3 cells/cm^2 onto the films and cultured in the growth medium containing 10% FBS.

For cell staining at each predetermined incubation time, the films were gently washed with prewarmed PBS, and the cells were fixed with 2.5% glutaraldehyde for 20 min, permeabilized with 0.1% Triton X-100 for 5 min, and blocked with 1% BSA for 20 min. Actin fibers and cell nuclei were stained with Alexa Fluor 488 phalloidin (Invitrogen, CA, USA) and 4′,6-diamidino-2-phenylindole (DAPI) (Invitrogen, CA, USA), respectively. Fluorescence images were then taken with an inverted fluorescence microscope (IX-71, Olympus). Cell proliferation was evaluated by direct cell counting using fluorescence images taken in five random fields per surface.

2.5. MTT Assay. At predetermined cell-incubation times the films were gently washed with prewarmed PBS and transferred into new wells which contained 0.2 mL fresh medium and 0.02 mL MTT (5 mg/mL in 0.1 M PBS). After incubation at 37 °C for 4−5 h, the medium was carefully removed and the purple colored product was dissolved in 0.2 mL dimethyl sulfoxide (DMSO). 0.1 mL of the solution was transferred to new wells, and the absorbance at 550 nm was determined (Thermo Scientific Varioskan Flash). Absorbance was taken as proportional to cell viability.

2.6. Statistical Analysis. Wettability, protein adsorption, cell number, and cell viability on films were expressed as mean ± standard deviation (SD) and analyzed by one-way analysis of variance (ANOVA). $p < 0.05$ was considered statistically significant.

3. RESULTS AND DISCUSSION

3.1. Lotus-leaf-like Topography of PHBHHx-L Surface. PHBHHx films with lotus-leaf-like topography (PHBHHx-L) were fabricated by replica molding as described. Typical SEM micrographs of the films are shown in Figure 1. The surface consists of an array of micro papillae of diameter 7.6 ± 1.3 μm and height 10.7 ± 2.8 μm. These are distributed evenly on the PHBHHx-L surface (Figure 1A, B). The surfaces of the papillae

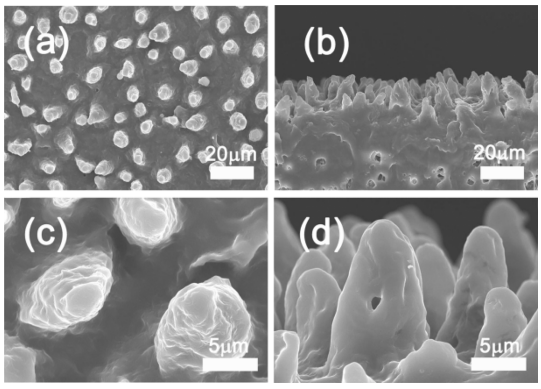

Figure 1. Scanning electron microcopy images of PHBHHx with lotus-leaf-like topography (PHBHHx-L). (A, C) Top view and (B, D) side view. Scale bars: (A, B) 20 μm, (C, D) 5 μm.

are covered with smaller structures (Figures 1C, D). It has been reported that the roughness factor of lotus leaf replica is 1.7, as evaluated by white light profilometry.[24] On the basis of the definition of roughness factor, i.e., the ratio of the true area to the apparent area, the true surface area of PHBHHx-L is about 1.7 times the surface area of PHBHHx-F.

3.2. Wettability of Lotus-leaf-like PHBHHx Surface. Surface topography has a major influence on surface wettability.[25] In this study, the wettability of the PHBHHx-F and PHBHHx-L surfaces was investigated by measuring advancing and receding water contact angles. As shown in Figure 2, the advancing and receding contact angles for

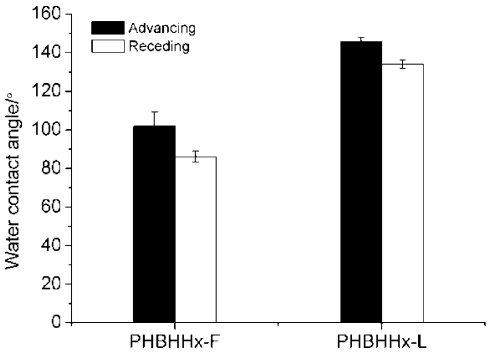

Figure 2. Advancing and receding water contact angles of the flat PHBHHx-F and lotus-leaf-like PHBHHx-L surfaces. Data are mean ± SD (n = 3).

PHBHHx-F were 102 ± 7 and 86.2 ± 3°, respectively. When lotus-leaf-like topography was introduced, the advancing and receding angles increased to 146 ± 2 and 134 ± 2°, respectively, showing that the hydrophobicity of the PHBHHx surface was enhanced significantly because of the introduction of the lotus-leaf-like structure.

3.3. Protein Adsorption. Protein adsorption on a material surface can be influenced by surface topography.[26] In this study, Fg was used as a model protein to investigate nonspecific protein adsorption on the PHBHHx surfaces. As shown in Figure 3, Fg adsorption on the PHBHHx-L and PHBHHx-F surfaces was 0.64 ± 0.04 μg and 0.39 ± 0.05 μg, respectively (per disc basis). The ratio of the adsorbed quantities, 1.64, is close to the ratio of the true surface areas, indicating that the higher adsorption on the lotus-leaf-like PHBHHx surface is mainly attributable to the increased surface area.

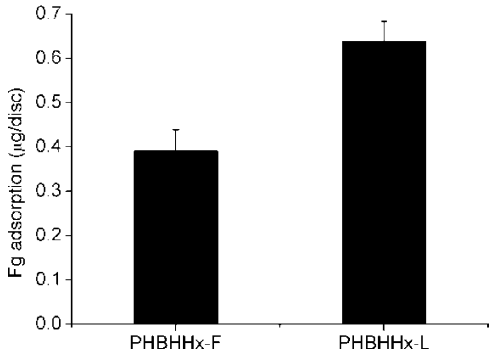

Figure 3. Fibrinogen adsorption on the flat (PHBHHx-F) and lotus-leaf-like (PHBHHx-L) surfaces. The "apparent" surface area of each disc is about 0.32 cm^2. Data are mean ± SD (n = 3).

It is generally considered that cell−surface interactions are mediated by the extracellular matrix proteins.[27−30] Fn and Vn are two primary extracellular matrix proteins that mediate cell adhesion[31] and the adsorption of these proteins on a surface may be predictive of the extent of cell-surface interactions.[32,33] In this study, Fn and Vn adsorption from cell culture medium was measured by ELISA. As seen in Figure 4, compared with

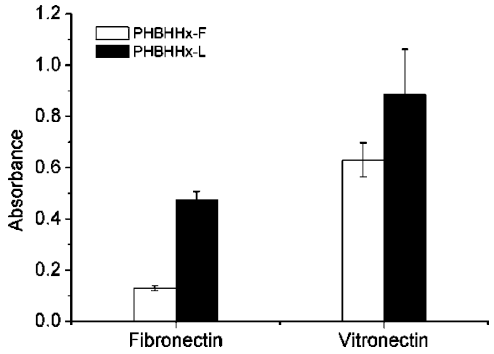

Figure 4. Adsorption of Fn and Vn from cell culture medium measured by ELISA. Data are mean ± SD (n = 3).

flat PHBHHx, adsorption on the PHBHHx-L surface increased by ∼260% for Fn and ∼40% for Vn, again presumably due to the greater surface area of the lotus-leaf-like surface. It should be noted that protein adsorption in cell culture medium is quite complicated due to the competitive adsorption. This may be the main reason why the ratio of Fn/Vn adsorption on PHBHHx-L and PHBHHx-F doesn't coincide with that for Fg adsorption.

3.4. Cell Interaction. Cell adhesion and proliferation on a material surface may be influenced indirectly by adsorbed extracellular matrix proteins and directly by surface topography. To investigate the contributions of these two factors to cell interactions with the PHBHHx surfaces, fibroblast and endothelial cell adhesion and proliferation were measured. Cell densities on the material surfaces at different culture times are shown in Figure 5. The densities of both cell types increased with culture time on both the flat and the lotus-leaf-like surfaces. In the case of fibroblasts, the densities on the two surfaces were the same over the 7 days of the experiment (p > 0.2, Figure 5a), while for endothelial cells, the density on the PHBHHx-L surface was significantly lower than on the PHBHHx-F surface at 5 and 7 days (Figure 5b). It is interesting that although the PHBHHx-L surface adsorbed

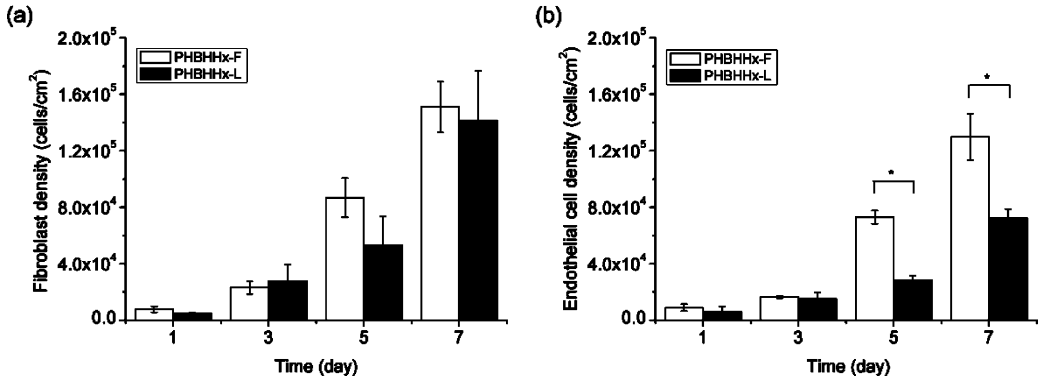

Figure 5. Cell densities of (a) fibroblasts and (b) endothelial cells on the flat PHBHHx-F and the lotus-leaf-like PHBHHx-L surfaces at different culture times. Data are mean ± SD (n = 3), * p < 0.05.

greater quantities of cell-adhesive proteins than the PHBHHx-F, it did not support greater cell adhesion and proliferation; rather in the case of endothelial cells, proliferation was significantly lower on the lotus like surface. These data suggest that surface topography dominates over adsorbed ECM protein adsorption for cell adhesion and proliferation on the lotus-leaf-like PHBHHx surface.

The morphologies of fibroblasts and endothelial cells on the PHBHHx surfaces are shown in Figure 6. On the PHBHHx-F

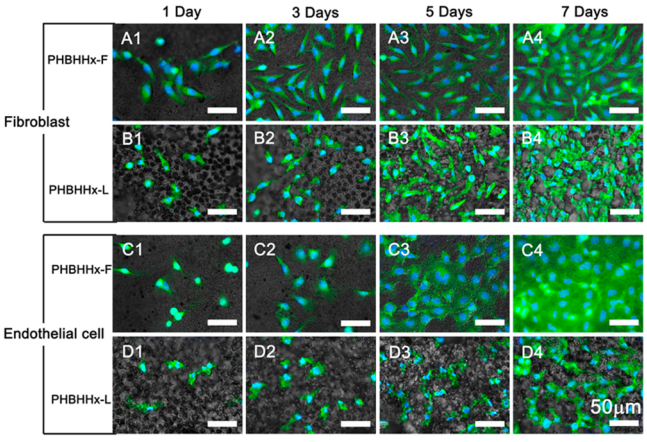

Figure 6. Fluorescence microscope images of stained fibroblasts and endothelial cells on the flat PHBHHx-F and the lotus-leaf-like PHBHHx-L surfaces. To view the cells and the underlying substratum, we acquired images in bright field and in fluorescence mode at the same focal length and merged. Scale bars are 50 μm.

surface, both fibroblasts and endothelial cells were well-spread and showed normal morphology (Figure 6A, C), indicating good cytocompatibility of PHBHHx.[20,34] On the PHBHHx-L surface, fibroblast spreading was restricted to some extent by the microscale topography, although most of the cells adhered in the gaps between the micropapillae and showed fusiform morphology (Figure 6B). The spreading of endothelial cells on the PHBHHx-L surface was severely restricted and the cells were small and highly irregular in shape (Figure 6D). These data are in accordance with the cell counting results, indicating that the lotus-leaf-like topography is unfavorable for cell proliferation. In addition, it is evident that the effects of surface topography of PHBHHx-L on the different cell lines are not the same. Su et al. found that higher pillars (1−10 μm in height, 1 μm in diameter) promoted fibroblast attachment, but impeded normal cellular shape formation.[35] Although the height of the micropapillae on the lotus-leaf-like PHBHHx surface is about 10 μm, its diameter is much greater than 1 μm. As a result, the micropapillae cannot fix the cells on their top, and the cells spread into the gaps between the papillae. In the case of endothelial cells, Ranjan and Webster demonstrated that convex−concave structure with wider spacing (22−80 μm) favored cell adhesion;[36] Dickinson et al. demonstrated that micropillars of height >3 μm decreased endothelial cell adhesion and spreading significantly.[37] In the present study, the spacing between the papillae was less than 20 μm, and the height obviously exceeded 3 μm (Figure 1). This may explain why endothelial cells did not grow normally on the lotus-leaf-like PHBHHx surface. In addition, endothelial cells usually assume a rounded shape in vitro, whereas the fibroblasts are elongated with abundant protrusions and filopodia.[38] Thus the narrow, "winding" grooves formed by the micropapillae seem more favorable for the elongated fibroblasts than for the endothelial cells. The morphology of the cells is thus also important in the interactions of cells with "topographic" surfaces.

3.5. MTT Assay. The MTT assay provides an indication of cell viability. As seen in Figure 7, changes in viability on the surfaces with culture time for the two cell lines showed trends similar to cell density (Figure 5) and cell spreading (Figure 6), suggesting that cell density and cell spreading are the main determinants of cell viability. On both the flat and lotus-leaf-like surfaces, cell viability increased with culture time, indicating that cells were proliferating. The viability of fibroblasts on the PHBHHx-F and the PHBHHx-L surfaces was the same over the time course of the experiment (p > 0.1, Figure 7a), whereas endothelial cells were less viable on the PHBHHx-L surface than on the PHBHHx-F surface at days 5 and 7. Moreover, the difference in cell viability on the two surfaces increased with time (Figure 7b). As shown in Figures 5 and 6, the density and spreading of endothelial cells on the PHBHHx-L surface were restricted; this may explain why cell viability was impaired on the lotus-leaf-like surface.

Cell−surface interactions are complicated. Surface properties such as topography and chemistry, and protein adsorption may all influence cell behavior on the surface. In addition, different cell lines may behave differently on the same surface. In the present study, both fibroblasts and endothelial cells adhered well and spread on the flat PHBHHx-F surface, indicating that the surface chemistry of PHBHHx is favorable for cell growth. Adsorption of cell-adhesive proteins was shown to be greater

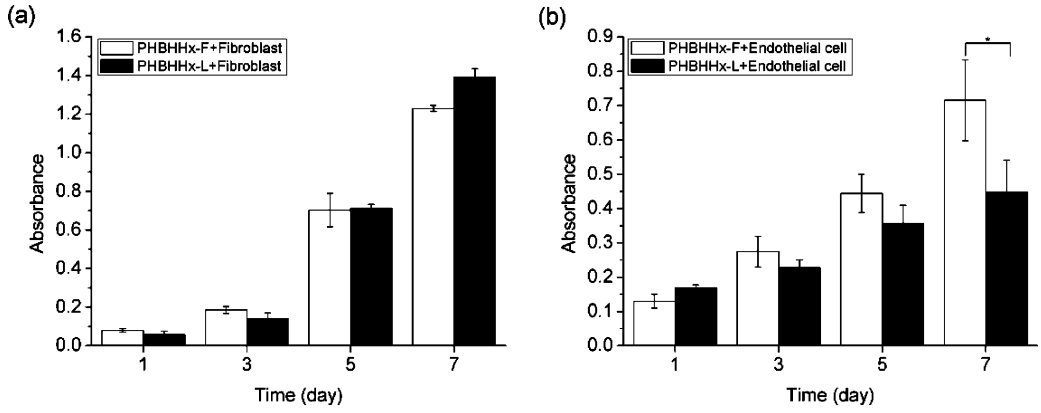

Figure 7. Viability of (a) fibroblasts and (b) endothelial cells on the flat PHBHHx-F and the lotus-leaf-like PHBHHx-L surfaces at different culture times measured by MTT assay. Data are mean ± SD (n = 3), * p < 0.05.

on PHBHHx-L than on PHBHHx-F, but cell proliferation on the PHBHHx-L surface was not greater than on PHBHHx-F. It can thus be concluded that the lotus-leaf-like topography does not promote the proliferation of fibroblasts and endothelial cells, and that this negative effect of topography plays a dominant role in cell/PHBHHx-L interactions. The lotus-leaf-like topography showed different degrees of inhibition of proliferation for the two cell lines, and endothelial cells were more inhibited than fibroblasts.

4. CONCLUSION

In this work, a lotus-leaf-like PHBHHx polymer surface was fabricated by replica molding and was used to investigate the effect of the special lotus leaf topography on cell adhesion and proliferation. The influence of adsorbed extracellular matrix proteins was also studied. Adsorption of the extracellular matrix proteins (Fn and Vn) was greater on the lotus-leaf-like surface than on the flat polymer surface; this is mainly attributed to the greater surface area of the lotus-leaf-like surface. In contrast, cell proliferation was not greater on the lotus-like topography, and indeed was lower on the lotus-like surface than on the flat surface. It is concluded that lotus-leaf-like topography predominates over adsorbed ECM proteins in PHBHHx-L/cell interactions. In addition, the lotus-leaf-like topography showed different degrees of proliferation inhibition for the two cell lines, and the proliferation of endothelial cells was more inhibited than that of fibroblasts.

AUTHOR INFORMATION

Corresponding Author

*Tel: +86-512-65880527 (D.L.); +86-512-65880827 (H.C.). Fax: +86-512-65880583 (D.L.); +86-512-65880583 (H.C.). E-mail: lidan@suda.edu.cn (D.L.); chenh@suda.edu.cn (H.C.).

Notes

The authors declare no competing financial interest.

ACKNOWLEDGMENTS

This work was supported by the National Natural Science Foundation of China (21204055), the National Science Fund for Distinguished Young Scholars (21125418), the Project of Scientific and Technologic Infrastructure of Suzhou (SZS201207), and the Priority Academic Program Development of Jiangsu Higher Education Institutions (PAPD). We thank Professor Guoqiang Chen from Tsinghua University for kindly providing PHBHHx and Professor John Brash from McMaster University for helpful discussions.

REFERENCES

(1) Hay, E. D. *J. Cell Biol.* **1981**, *91*, 205−223.
(2) Bosman, F. T.; Stamenkovic, I. *J. Pathol.* **2003**, *200*, 423−428.
(3) Stevens, M. M.; George, J. H. *Science* **2005**, *310*, 1135−1138.
(4) Friedl, P.; Bröcker, E. B. *Cell. Mol. Life Sci.* **2000**, *57*, 41−64.
(5) Goodman, S. L.; Sims, P. A.; Albrecht, R. M. *Biomaterials* **1996**, *17*, 2087−2095.
(6) Rørth, P. *Dev. Cell* **2011**, *20*, 9−18.
(7) Roach, P.; Eglin, D.; Rohde, K.; Perry, C. *J. Mater. Sci.: Mater. Med.* **2007**, *18*, 1263−1277.
(8) Shi, X. J.; Wang, Y. Y.; Li, D.; Yuan, L.; Zhou, F.; Wang, Y. W.; Song, B.; Wu, Z. Q.; Chen, H.; Brash, J. L. *Langmuir* **2012**, *28*, 17011−17018.
(9) Deligianni, D.; Katsala, N.; Ladas, S.; Sotiropoulou, D.; Amedee, J.; Missirlis, Y. *Biomaterials* **2001**, *22*, 1241−1251.
(10) Chen, H.; Song, W.; Zhou, F.; Wu, Z. K.; Huang, H.; Zhang, J. H.; Quan, L.; Yang, B. *Colloids Surf., B* **2009**, *71*, 275−281.
(11) Schulte, V. A.; Díez, M.; Möller, M.; Lensen, M. C. *Biomacromolecules* **2009**, *10*, 2795−2801.
(12) Papenburg, B. J.; Rodrigues, E. D.; Wessling, M.; Stamatialis, D. *Soft Matter* **2010**, *6*, 4377−4388.
(13) Charest, J. L.; Eliason, M. T.; García, A. J.; King, W. P. *Biomaterials* **2006**, *27*, 2487−2494.
(14) Zhou, F.; Li, D.; Wu, Z. Q.; Song, B.; Yuan, L.; Chen, H. *Macromol. Biosci.* **2012**, *12*, 1391−1400.
(15) Zheng, J.; Song, W.; Huang, H.; Chen, H. *Colloids Surf., B* **2010**, *77*, 234−239.
(16) Le Saux, G.; Magenau, A.; Böecking, T.; Gaus, K.; Gooding, J. J. *PLoS One* **2011**, *6*, e21869.
(17) Wang, P. Y.; Thissen, H.; Tsai, W. B. *Biotechnol. Bioeng.* **2012**, *109*, 2104−2115.
(18) Wang, Y. W.; Mo, W.; Yao, H.; Wu, Q.; Chen, J.; Chen, G. Q. *Polym. Degrad. Stab.* **2004**, *85*, 815−821.
(19) Qu, X. H.; Wu, Q.; Zhang, K. Y.; Chen, G. *Biomaterials* **2006**, *27*, 3540−3548.
(20) Wang, Y. W.; Yang, F.; Wu, Q.; Cheng, Y.; Yu, P. H. F.; Chen, J.; Chen, G. Q. *Biomaterials* **2005**, *26*, 755−761.
(21) Wang, Y.; Bian, Y. Z.; Wu, Q.; Chen, G. Q. *Biomaterials* **2008**, *29*, 2858−2868.
(22) Chen, G. Q.; Wu, Q. *Biomaterials* **2005**, *26*, 6565−6578.
(23) Wagner, M. S.; Horbett, T. A.; Castner, D. G. *Biomaterials* **2003**, *24*, 1897−1908.
(24) Spori, D. M.; Drobek, T.; Zürcher, S.; Ochsner, M.; Sprecher, C.; Mühlebach, A.; Spencer, N. D. *Langmuir* **2008**, *24*, 5411−5417.
(25) Blossey, R. *Nat. Mater.* **2003**, *2*, 301−306.
(26) Song, W.; Chen, H. *Chin. Sci. Bull.* **2007**, *52*, 3169−3173.

(27) Keselowsky, B. G.; Collard, D. M.; García, A. J. *J. Biomed. Mater. Res.* **2003**, *66A*, 247−259.
(28) Hersel, U.; Dahmen, C.; Kessler, H. *Biomaterials* **2003**, *24*, 4385−4415.
(29) García, A. J.; Boettiger, D. *Biomaterials* **1999**, *20*, 2427−2433.
(30) Chen, H.; Yuan, L.; Song, W.; Wu, Z. K.; Li, D. *Prog. Polym. Sci.* **2008**, *33*, 1059−1087.
(31) Steele, J. G.; Johnson, G.; Norris, W. D.; Underwood, P. A. *Biomaterials* **1991**, *12*, 531−539.
(32) Woo, K. M.; Seo, J.; Zhang, R.; Ma, P. X. *Biomaterials* **2007**, *28*, 2622−2630.
(33) Woo, K. M.; Chen, V. J.; Ma, P. X. *J. Biomed. Mater. Res.* **2003**, *67A*, 531−537.
(34) Qu, X. H.; Wu, Q.; Chen, G. Q. *J. Biomater. Sci., Polym. Ed.* **2006**, 171107−1121.
(35) Su, W. T.; Liao, Y. F.; Lin, C. Y.; Li, L. T. *J. Biomed. Mater. Res. A* **2010**, *93A*, 1463−1469.
(36) Ranjan, A.; Webster, T. J. *Nanotechnology* **2009**, *20*, 305102−305112.
(37) Dickinson, L. E.; Rand, D. R.; Tsao, J.; Eberle, W.; Gerecht, S. *J. Biomed. Mater. Res. A* **2012**, *100A*, 1457−1466.
(38) Biela, S. A.; Su, Y.; Spatz, J. P.; Kemkemer, R. *Acta Biomater.* **2009**, *20*, 2460−2466.